Analyst

PAPER

View Article Online
View Journal | View Issue

Cite this: *Analyst*, 2015, **140**, 7912

Polythiophene derivative on quartz resonators for miRNA capture and assay†

Al. Palaniappan,*[a,b] Jamal Ahmed Cheema,[a,b] Deepa Rajwar,[a,b] Gopal Ammanath,[a,b,c] Liu Xiaohu,[a,b] Lim Seng Koon,[a,b] Wang Yi,[a,b] Umit Hakan Yildiz[d,e] and Bo Liedberg*[a,b]

Received 14th August 2015,
Accepted 4th October 2015

DOI: 10.1039/c5an01663k

www.rsc.org/analyst

A novel approach for miRNA assay using a cationic polythiophene derivative, poly[3-(3′-*N*,*N*,*N*-triethylamino-1′-propyloxy)-4-methyl-2,5-thiophene hydrobromide] (PT), immobilized on a quartz resonator is proposed. The cationic PT enables capturing of all RNA sequences in the sample matrix *via* electrostatic interactions, resulting in the formation of PT–RNA duplex structures on quartz resonators. Biotinylated peptide nucleic acid (b-PNA) sequences are subsequently utilized for the RNA assay, upon monitoring the PT–RNA–b-PNA triplex formation. Signal amplification is achieved by anchoring avidin coated nanoparticles to b-PNA in order to yield responses at clinically relevant concentration regimes. Unlike conventional nucleic acid assay methodologies that usually quantify a specific sequence of RNA, the proposed approach enables the assay of any RNA sequence in the sample matrix upon hybridization with a PNA sequence complementary to the RNA of interest. As an illustration, successful detection of mir21, (a miRNA sequence associated with lung cancer) is demonstrated with a limit of detection of 400 pM. Furthermore, precise quantification of mir21 in plasma samples is demonstrated without requiring PCR and sophisticated instrumentation.

Introduction

Over the past few years, optical properties of conjugated polyelectrolytes (CPEs) have been exploited for applications in nucleic acid assays.[1–9] The assays are based on changes in the optical properties of CPEs that are attributed to the polymer backbone conformation. Upon interaction with nucleic acids, positively charged CPEs form a complex and exhibit changes in colorimetric and fluorometric signals that are enhanced by a collective response. Recent studies have revealed that optical property changes could even facilitate the naked eye detection of nucleic acids.[7–12] However, solution based methodologies often encounter difficulties due to uncontrolled complexation, therefore limiting the selectivity of the nucleic acid assay.[13] Moreover, most of the approaches do not yield quantitative analysis without inclusion of sophisticated optical characterization techniques. Optical methods further have limitations to perform a quantitative nucleic acid assay in complex samples, for instance serum. Furthermore, there is a need for a "mix-and-measure" type assay to detect fragile gene fragments as well as microRNA (miRNA) sequences. Therefore, spirited by the recent advances in programmable complex formation upon impregnation of CPEs on paper based solid substrates,[14] we have attempted to utilize a polythiophene derivative which is a cationic CPE, for the first time, as a responsive layer on a resonator platform such as a quartz crystal microbalance (QCM) for specific and quantitative analysis of miRNA. In this report, the cationic polythiophene derivative, poly[3-(3′-*N*,*N*,*N*-triethylamino-1′-propyloxy)-4-methyl-2,5-thiophene hydrobromide] (PT), is immobilized on the QCM surface for capturing miRNA *via* electrostatic interactions.

Cationic PTs are utilized for maximizing the interaction with negatively charged nucleic acids.[8,9] They freely form hydrogels with significant swelling at physiological pH facilitating complete capture of miRNA.[15] As reported previously, PT complexes with miRNA *via* electrostatic interactions yielding a duplex structure.[14,16] PT therefore captures the target miRNA and other interfering miRNAs in complex samples. Triplex formation or specific detection is achieved upon injection of a PNA sequence complementary to the target miRNA. mir21, a miRNA sequence associated with lung cancer, is utilized in the study for validation of the proposed approach.

[a]*School of Materials Science and Engineering, Nanyang Technological University, Singapore 639798. E-mail: alps@ntu.edu.sg, bliedberg@ntu.edu.sg; Fax: +65 67909081; Tel: +65 6513 7352*
[b]*Center for Biomimetic Sensor Science, 50 Nanyang Drive, Singapore 637553*
[c]*Nanyang Institute of Technology in Health and Medicine, Interdisciplinary Graduate School, Nanyang Technological University, Singapore 637553*
[d]*Department of Chemistry, Izmir Institute of Technology, 35430, Urla, Izmir, Turkey*
[e]*Stanford University School of Medicine, Palo Alto, California 94304, USA*
†Electronic supplementary information (ESI) available. See DOI: 10.1039/c5an01663k

Several assay formats based on QCM have been reported, usually involving a recognition molecule immobilized on the QCM crystal surface that can specifically bind a target analyte.[17–19] As for the nucleic acid assay, PNA/DNA probes are usually immobilized on the QCM surface for detection of a particular DNA/RNA sequence of interest. Though sub-pM detection sensitivities have been reported based on QCM,[18,19] most of the reports possess the limitation of quantifying a specific sequence of RNA in the sample matrix. Unlike conventional nucleic acid probes that are immobilized on the QCM surface, PT, proposed in this study, enables capturing all miRNAs in a sample matrix, providing a unique possibility of detecting any miRNA sequence upon injection of a peptide nucleic acid (PNA) sequence complementary to the miRNA of interest. Avidin coated nanoparticles (ANPs) are subsequently utilized for signal amplification and to yield responses in clinically relevant concentration regimes. Avidin functionalized nanoparticles selectively bind to the biotin anchored to PNA. ANPs serve as mass enhancers amplifying the PNA hybridization signal. QCM frequency shift responses are then directly correlated with the miRNA concentration, thereby eliminating the need for PCR upon miRNA isolation.

Experimental

All the chemicals for PT synthesis were purchased from Sigma–Aldrich and used without further purification. Deionized (DI) MilliQ water (resistivity of 18 MΩ cm) was used for buffer preparation and PT synthesis. Precursors **1** and **2** were synthesized according to previous reports.[20] Quaternization of precursor **2** with triethylamine yielded monomer **1**. PT was subsequently synthesized by oxidative polymerization of monomer **1** (Scheme 1). The structures of the precursors and monomers were confirmed by NMR spectroscopy. The number averaged molecular weight of the synthesized PT is estimated to be between 6 and 10 kDa.[21] Similarly, PT with a varying pendant group was synthesized in order to investigate/optimize its interaction with miRNA (Fig. S1†). A Perkin Elmer Lambda 35 UV-vis spectrometer, Infinite M200Pro Tecan plate reader and Thermo Scientific Nanodrop 2000c Spectrophotometer were used for optical characterization of the synthesized PT, prior to applying the polymer in the QCM based assay.

5 MHz AT-cut piezoelectric quartz crystals coated with gold were obtained from Q-Sense, Sweden. QCM crystals were cleaned before use by first treating them with ozone for 10 min followed by sonication in 99% ethanol for 5 min. The crystals were then rinsed with ethanol followed by DI water and blown dry with N_2. The cleaned crystals were mounted in the microfluidic chamber of the Q-Sense instrument. Real time QCM measurements were carried out using Q-Sense E4. Upon attaining a stable resonant frequency, 250 μL of varying concentrations of PT was injected (at a flow rate of 50 μL min^{-1}) into the QCM chamber. An optimized concentration of 0.1 mg ml^{-1} based on polymer loading was chosen for the assay (Fig. S2†) to form a layer of ~2.8 nm thickness (Fig. S3†). PBS with 0.002% Tween (PBST) was used as a running buffer solution and for PNA/miRNA dilutions.

The following miRNA and PNA sequences were purchased from IDT and Panagene, respectively.

mir21: 5′-UAG CUU AUC AGA CUG AUG UUG A-3′

Non-complementary sequence (Nc): 5′-AUG CAU GCA UGC AUG CAU GCA A-3′

Biotinylated PNA sequence (b-PNA): biotin – OO – 5′ TCA ACA TCA GTC TGA TAA GCT A 3′, where O represents a glycol spacer.

miRNA stock solutions of 100 μM were prepared with RNase free DI water and stored at −20 °C. For miRNA assay, PT addition was followed by injections of 250 μL of bovine serum albumin (BSA, 5 mg ml^{-1}), 250 μL of miRNA (at a varying concentration), 250 μL of b-PNA and 0.1 mg ml^{-1} ANP. ANP, purchased from Chemicell GmbH, Germany, comprises of a magnetite core covered in a starch matrix and functionalized with avidin. The particles are of ~100 nm in size and suspended in PBS with 0.05% sodium azide buffer. Human plasma was purchased from GeneTex, Taiwan for spiking experiments, upon isolation of mir21 using Macherey-Nagel's Nucleospin miRNA extraction kit.

Results and discussion

Optical characterization of PT

In order to understand and validate PT as a responsive layer upon interaction with mir21, absorption and fluorescence spectra of 150 μM of PT in the presence and absence of 10 μM miRNA were recorded at room temperature. The UV–Vis absorption and emission maxima in DI water solution of PT have been observed at 403 nm and 537 nm, respectively. These peaks are due to the random coil morphology of the PT backbone and are in agreement with previous reports.[14,22–24] Fig. 1a

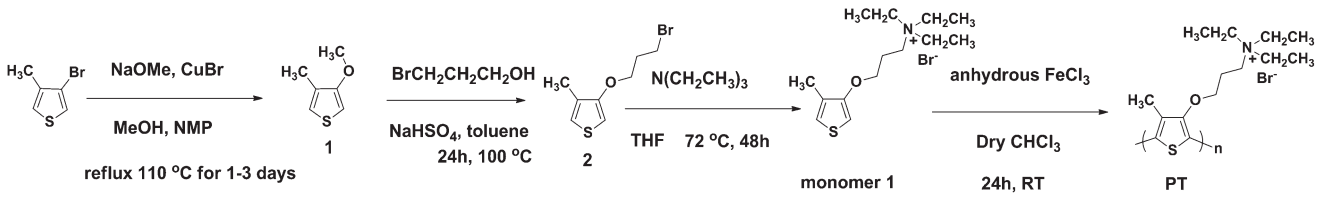

Scheme 1 Synthesis of PT.

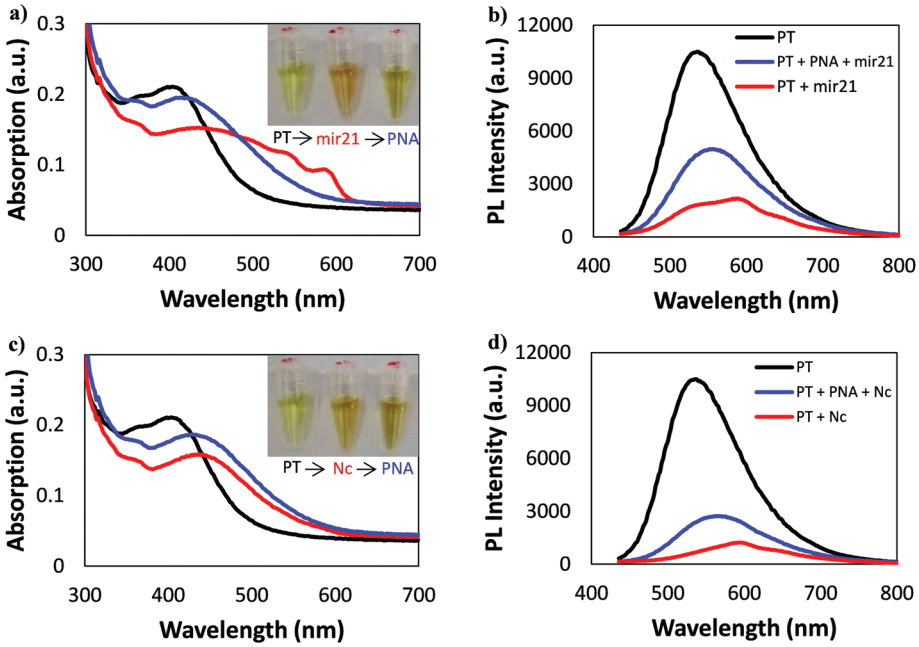

Fig. 1 (a, b) Absorption and emission spectra with images (inset a) of PT with subsequent addition of mir21 followed by PNA; (c, d) absorption and emission spectra with images (inset c) of PT with subsequent addition of the Nc sequence followed by PNA.

and c show red shifts from the main absorption peak (403 nm) upon addition of 30 μL of 10 μM mir21 and the Nc sequence (red curves), respectively. For the mir21, redistribution of the absorption spectrum with the main absorption peak at 442 nm, and two vibronic peaks at 541 nm and 589 nm was observed, whereas a single broad absorption curve with maxima at 439 nm was observed for Nc. This difference in the absorption peak is possibly because of the difference in the interaction mode of PT with mir21 and Nc, due to the very sensitive nature of the PT backbone (changing conformation from nonplanar to planar) towards different nucleotides. As reported previously, the red shift is attributed to PT–miRNA duplex formation governed by the electrostatic interactions between PT and miRNA sequences.[14] Fig. 1a shows that a prominent blue shift of the main absorption peak, ~30 nm, was observed for mir21 compared to the Nc sequence (Fig. 1c) upon addition of the PNA sequence complementary to mir21 (blue curve).

The fluorescence emission spectra show a significant quenching of PT fluorescence upon exposure to mir21 and Nc sequences. As observed from Fig. 1b and d, recovery of the fluorescence upon addition of PNA is significantly higher for mir21 in comparison with the Nc sequence, due to the change from planar to a non-planar "random" backbone of PT in the PT–PNA–mir21 triplex construct. The optical images of vials containing PT with mir21 and with Nc sequences (insets in Fig. 1a and c, respectively) indicate a similar colorimetric response for the two sequences. However, recovery in the colorimetric response is more evident for mir21 upon addition of a complementary PNA sequence, in agreement with the UV-Vis spectra (the red and blue curves in Fig. 1a and c). Fig. 1 ascertains that the optical shifts are consistent with the duplex/triplex formation and that the synthesized PT could be utilized as a responsive layer on QCM surface for miRNA assay. Herein, we explore the potential of immobilizing PT on QCM surfaces for specific and quantitative analysis of miRNA.

QCM assay

The proposed assay (Fig. 2) involves sequential injection of the synthesized PT and BSA into the QCM chamber, followed by miRNA and a complementary sequence of b-PNA for hybridization with the target miRNA sequence; ANPs are subsequently utilized for amplified detection of miRNA. PT was injected simultaneously into two chambers mounted with cleaned QCM crystals. Upon injection of PT, a two-step frequency response (Fig. 3(a) was observed) due to changes in the morphology of PT upon buffer exchange between DI water and PBST, in agreement with previous reports.[24] The surface mass coverage of the PT as revealed by SPR was estimated to be

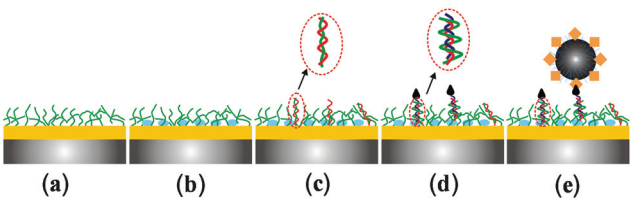

Fig. 2 Schematic illustration of the mir21 assay on QCM crystals. Quartz crystal is sequentially exposed to (a) PT, (b) BSA for gold substrate passivation, (c) RNA and duplex formation, (d) b-PNA and triplex formation, and (e) ANP for signal amplification.

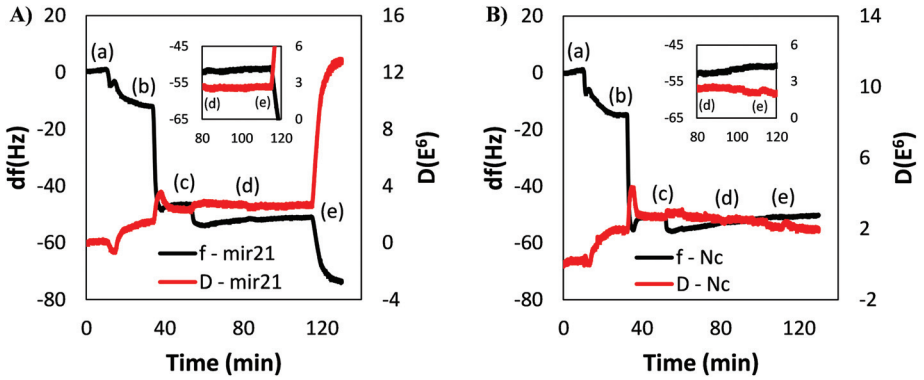

Fig. 3 QCM kinetic measurements: frequency (df) and energy dissipation (D) at the third overtone for (A) mir21 and (B) Nc sequence illustrating responses after the injection of (a) PT, (b) BSA, (c) 10 μM mir21/Nc sequence, (d) b-PNA, and (e) 0.1 mg ml^{-1} ANP.

~158 ng cm^{-2}; corresponding to a thickness of ~2.8 nm and a density of ~1.2 × 10^{13} molecules cm^{-2}, further indicating PT immobilization on the QCM surface (see Fig. S3† for experimental details). 5 mg ml^{-1} BSA in PBST was then injected for substrate passivation in order to minimize physisorption of ANP and other interfering species present in the complex matrices on Au surfaces (b), if any. 10 μM of mir21 and 10 μM of Nc sequences were then injected into chambers 1 and 2, respectively. Identical resonance frequency shifts of ~5 Hz (c) were obtained for both mir21 and Nc sequences indicating that the synthesized PT captures both Nc and mir21 sequences. 10 μM b-PNA complementary to mir21 was subsequently injected into both channels, followed by injection of ANP. Although no obvious frequency or dissipation shifts (0.5 Hz and 0.27E^6, respectively) were noticed upon b-PNA hybridization with mir21 (d), significant frequency and dissipation shifts (20 Hz and 10E^6, respectively) were observed upon injection of 0.1 mg ml^{-1} ANP (e). PNA–mir21–PT triplex formation is therefore ascertained as only a negligible shift was recorded for the Nc–PT duplex, indicating the successful capture of miRNA by PT immobilized on the Au surface and selective recognition of the mir21–PT duplex by b-PNA. As shown in Fig. 3, approximately 40-fold signal amplification, a shift of 20 Hz upon ANP addition for mir21 compared to ~0.5 Hz for Nc sequence, was achieved by injection of ANP.

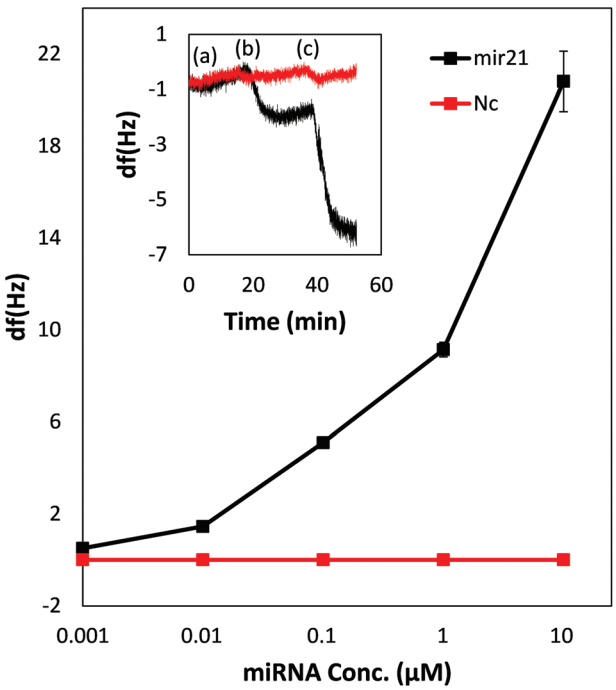

Fig. 4 Concentration dependent responses for mir21 and Nc sequences (n = 3). Inset: QCM kinetic measurement for mir21 and Nc sequences isolated from plasma (a) b-PNA, (b) 0.1 mg ml^{-1} ANP, and (c) 0.5 mg ml^{-1} ANP.

Selective detection of mir21

Concentration dependent responses (Fig. 4) reveal that frequency shifts were observed only when mir21 is captured by PT immobilized on the QCM surface. Almost negligible responses were obtained for all test concentrations of Nc sequence (curve Nc) indicating minimum interaction and binding between Nc and b-PNA (complementary to mir21)/ANP. A frequency shift of ~5 Hz was obtained for 100 nM of mir21 compared to ~0.5 Hz for 100 nM of the Nc sequence, illustrating that incorporation of capture and amplification methodologies enables selective detection of miRNA. Quantification of miRNA is subsequently achieved by correlating frequency responses with mir21 concentrations. As observed from Fig. 4, frequency responses were obtained for 1 nM to 10 μM mir21, with a limit of detection of 400 pM, calculated using $3\sigma/S$,[25] where σ is the standard deviation and S is the slope of the concentration response, derived at a lower linear response range [between 1 nM and 10 nM, Fig. 4]. Repeatable frequency responses for all test concentrations of mir21 and Nc (n = 3) were obtained indicating the homogeneity in PT adsorption on QCM surfaces. The proposed methodology therefore illustrates the potential for analysis of complex samples containing miRNA in the clinically relevant nM concentration ranges.[21,26,27]

mir21 assay in plasma

The mir21 assay was then carried out using plasma for demonstrating the applicability of the proposed approach for complex matrices. Plasma samples were spiked with 1 μM of mir21 to mimic clinical samples. Commercially available extraction kits were then used for miRNA isolation, in order to minimize the potential interference associated with physisorption of plasma components. mir21 isolation was carried out adopting the standard protocol shown in Fig. S4.† For control measurements, the same protocol was adopted for plasma samples spiked with 1 μM of the Nc sequence. UV-Vis analysis was carried out at each step of the isolation process to confirm mir21 and Nc sequence extraction from the plasma samples (Fig. S5†). The inset in Fig. 4 shows a negligible shift for the plasma sample spiked with mir21 and Nc sequences upon injection of b-PNA (a). Following the injection of 0.1 mg ml^{-1} ANP, a frequency shift of ~2 Hz was observed for mir21 spiked plasma samples (b) compared to a negligible shift for the plasma samples spiked with the Nc sequence. The experimental results indicate that amplification enhancement could be achieved upon increasing the concentration of ANP. A further increase in the frequency response ~4 Hz (c) was observed upon injection of 0.5 mg ml^{-1} ANP to the plasma sample spiked with mir21. However, as observed from Fig. 4 inset, the increasing concentration of ANP resulted in higher signal to noise ratios. Further studies will therefore focus on optimization of assay and amplification protocols, emphasizing on the sensitivity and selectivity enhancement, for instance, tailoring the terminal groups of PT for maximizing the RNA capture and assay. Nevertheless, the proposed capture methodology enabled quantification of mir21 in plasma samples without requiring PCR and sophisticated instrumentation.

Conclusion

A cationic polythiophene derivative has been deposited on a quartz resonator such as QCM for mir21 assay using b-PNA and ANP amplification. The proposed methodology provides an approach to capture all miRNA sequences in the sample compared to conventional assays that quantify a specific sequence of RNA. Successful detection of mir21 was carried out at clinically relevant concentrations with a limit of detection of 400 pM. Since QCM offers portability, the proposed methodology is feasible for the development of point of care devices. Furthermore, the assay of other RNA sequences of interest could be carried out upon utilization of appropriate complementary PNA sequences.

Acknowledgements

The authors wish to acknowledge the research grant [Academic Research Fund (AcRF) Tier 1 MOE] from Nanyang Technological University, Singapore, to conduct this study.

References

1 B. Liu and G. C. Bazan, *Chem. Mater.*, 2004, **16**, 4467–4476.
2 A. C. Carreon, W. L. Santos, J. B. Matson and R. C. So, *Polym. Chem.*, 2014, **5**, 314–317.
3 W. Zheng and L. He, *Biomater. Sci.*, 2014, **2**, 1471–1479.
4 W. Zheng and L. He, *J. Am. Chem. Soc.*, 2009, **131**, 3432–3433.
5 B. Fang, S. Jiao, M. Li, Y. Qu and X. Jiang, *Biosens. Bioelectron.*, 2008, **23**, 1175–1179.
6 K. P. R. Nilsson and O. Inganäs, *Nat. Mater.*, 2003, **2**, 419–424.
7 H. A. Ho, A. Najari and M. Leclerc, *Acc. Chem. Res.*, 2008, **41**, 168–178.
8 H. A. Ho, M. Boissinot, M. G. Bergeron, G. Corbeil, K. Dore, D. Boudreau and M. Leclerc, *Angew. Chem., Int. Ed.*, 2002, **41**, 1548–1551.
9 Y. Zhang, Z. Li, Y. Cheng and X. Lv, *Chem. Commun.*, 2009, 3172–3174.
10 S. W. Thomas, G. D. Joly and T. M. Swager, *Chem. Rev.*, 2007, **107**, 1339–1386.
11 H. Jiang, P. Taranekar, J. R. Reynolds and K. S. Schanze, *Angew. Chem., Int. Ed.*, 2009, **48**, 4300–4316.
12 A. Najari, A. H. Ho, J. F. Gravel, P. Nobert, D. Boudreau and M. Leclerc, *Anal. Chem.*, 2006, **78**, 7896–7899.
13 K. Lee, L. K. Povlich and J. Kim, *Analyst*, 2010, **135**, 2179–2189.
14 U. H. Yildiz, A. Palaniappan and B. Liedberg, *Anal. Chem.*, 2013, **85**, 820–824.
15 P. Åsberg, P. Björk, F. Höök and O. Inganäs, *Langmuir*, 2005, **21**, 7292–7298.
16 K. Dore, S. Dubus, H. A. Ho, I. Levesque, M. Brunette, G. Corbeil, M. Boissinot, G. Boivin, M. G. Bergeron, D. Boudreau and M. Leclerc, *J. Am. Chem. Soc.*, 2004, **126**, 4240–4244.
17 K. A. Marx, *Biomacromolecules*, 2003, **4**, 1099–1120.
18 J. Wan, X. Liu, Y. Zhang, Q. Gao, H. Qi and C. Zhang, *Sens. Actuators, B*, 2015, **213**, 409–416.
19 Z. Ge, M. Lin, P. Wang, H. Pei, J. Yan, J. Shi, Q. Huang, D. He, C. Fan and X. Zuo, *Anal. Chem.*, 2014, **86**, 2124–2130.
20 C. Li, M. Numata, A. H. Bae, K. Sakurai and S. Shinkai, *J. Am. Chem. Soc.*, 2005, **127**, 4548–4549.
21 P. S. Mitchell, R. K. Parkin, E. M. Kroh, B. R. Fritz, S. K. Wyman, E. L. Pogosova-Agadjanyan, A. Peterson, J. Noteboom, K. C. O'Briant, A. Allen, D. W. Lin, N. Urban, C. W. Drescher, B. S. Knudsen, D. L. Stirewalt, R. Gentleman, R. L. Vessella, P. S. Nelson, D. B. Martin and M. Tewari, *Proc. Natl. Acad. Sci. U. S. A.*, 2008, **105**, 10513–10518.
22 Z. Liu, H. L. Wang and M. Cotlet, *Chem. Commun.*, 2014, **50**, 11311–11313.
23 B. Liu and G. C. Bazan, *J. Am. Chem. Soc.*, 2004, **126**, 1942–1943.
24 E. Li, L. Lin, L. Wang, M. Pei, J. Xu and G. Zhang, *Macromol. Chem. Phys.*, 2012, **213**, 887–892.

25 L. Torsi, G. M. Farinola, F. Merinelli, M. C. Tanese, O. H. Omar, L. Valli, F. Babudri, F. Palmisano, P. G. Zambonin and F. Naso, *Nat. Mater.*, 2008, **7**, 412–417.
26 S. Catuogno, C. L. Esposito, C. Quintavalle, L. Cerchia, G. Condorelli and V. Franciscis, *Cancers*, 2011, **3**, 1887–1898.
27 X. Pan, Z. Wang and R. Wang, *Cancer Biol. Ther.*, 2010, **10**, 1224–1232.